Synthesis of Colloidal Crystals of Controllable Thickness through the Langmuir−Blodgett Technique

Stéphane Reculusa* and Serge Ravaine

Centre de Recherche Paul Pascal−CNRS, 115, avenue du Dr Schweitzer, 33600 Pessac, France

Received June 25, 2002. Revised Manuscript Received November 11, 2002

Colloidal crystals of various thicknesses were obtained using silica particles as basic units and the Langmuir−Blodgett technique as a tool for controlling the thickness. Submicronic silica particles are first synthesized via a sol−gel process and then functionalized with an appropriate coupling agent. After compression at the surface of a Langmuir trough to form a well-organized two-dimensional array, silica particles are transferred onto solid substrates. While repeating the transfer several times, we formed colloidal crystals that were characterized by scanning electron microscopy and UV−visible−NIR spectroscopies. Both techniques show that the sample thickness can be controlled at the layer level whereas the overall crystal quality should be good enough for use in several applications.

Introduction

For many years, colloidal crystals have drawn a considerable interest in the field of materials chemistry, both for theoretical and experimental considerations. Such nanostructured materials, consisting of a controlled assembly of monodisperse colloids in a highly regular structure (typically a face-centered cubic system), are indeed particularly interesting and perfectly adequate for the field of photonic crystals, that is, dielectric materials with a one-, two-, or three-dimensional periodicity exhibiting peculiar interactions with light.[1−4] Since they can lead to porous materials,[5−8] other applications such as catalysis supports[9] (due to their high surface/volume ratio) or selective membranes[10] (size of voids in the crystal is tunable while adjusting the diameter of the templating particles) are also often described. To obtain these porous structures, colloidal crystals are usually first immersed in a solution of metallic precursors (like gold nanocrystals[11] or titanium alkoxides[12]) or monomers[13] and are submitted, after appropriate reactions that generate the material itself, to several treatments for removal of the templating particles (like calcination for polymers beads, etching with hydrofluoric acid for silica particles).

In the most recent developments, techniques of synthesis of colloidal crystals have been explored widely. Electrophoretic deposition,[14,15] sedimentation,[16] solvent evaporation,[17,18] or dipping[19,20] are examples of processes leading to such particulate assemblies. Taking advantage of the dynamic thin laminar flow (DTLF) method, Picard also described the elaboration of 2D crystals with polystyrene particles that could also lead to 3D structures.[21]

Naturally, each technique has its advantages and drawbacks, some being very easy to perform but very slow, some others being very convenient and fast but with worse control of the quality of the crystal.

In the present work, we aim to demonstrate that three-dimensional colloidal crystals can easily and rapidly be synthesized via the Langmuir−Blodgett (LB) technique, as shown previously by van Duffel et al. for two-dimensional systems,[22] with a perfectly controllable thickness. First, silica particles with a narrow size distribution are synthesized following a procedure inspired from previous works in the literature.[23,24] Then,

* To whom correspondence should be addressed. E-mail: reculusa@crpp.u-bordeaux.fr.

(1) Ozin, G. A.; Yang, S. M. *Adv. Funct. Mater.* **2001**, *11*, 95−104.
(2) Polman, A.; Wiltzius, P. *MRS Bull.* **2001**, 608−613.
(3) Noda, S. *Physica B* **2000**, *279*, 142−149.
(4) Blanco, A.; Chomski, E.; Grabtchak, S.; Ibisate, M.; John, S.; Leonard, S. W.; Lopez, C.; Meseguer, F.; Miguez, H.; Mondia, J. P.; Ozin, G. A.; Toader, O.; van Driel, H. M. *Nature* **2000**, *405*, 437−440.
(5) Velev, O. D.; Lenhoff, A. M. *Curr. Opin. Colloid Interface Sci.* **2000**, *5*, 56−63.
(6) Braun, P. V.; Wiltzius, P. *Curr. Opin. Colloid Interface Sci.* **2002**, *7*, 116−123.
(7) Jiang, P.; Hwang, K. S.; Mittleman, D. M.; Bertone, J. F.; Colvin, V. L. *J. Am. Chem. Soc.* **1999**, *121*, 11630−11637.
(8) Velev, O. D.; Jede, T. A.; Lobo, R. F.; Lenhoff, A. M. *Chem. Mater.* **1998**, *10*, 3597−3602.
(9) Schroden, R. C.; Blanford, C. F.; Melde, B. J.; Johnson, B. J. S.; Stein, A. *Chem. Mater.* **2001**, *13*, 1074−1081.
(10) Gates, B.; Yin, Y.; Xia, Y. *Chem. Mater.* **2001**, *11*, 2827−2836.
(11) Jiang, P.; Cizeron, J.; Bertone, J. F.; Colvin, V. L. *J. Am. Chem. Soc.* **1999**, *121*, 7957−7958.
(12) Wijnhoven, J. E. G. J.; Bechger, L.; Vos, W. L. *Chem. Mater.* **2001**, *13*, 4486−4499.
(13) Johnson, S. A.; Ollivier, P. J.; Mallouk, T. E. *Science* **1999**, *283*, 963−965.
(14) Holgado, M.; Garcia-Santamaria, F.; Blanco, A.; Ibisate, M.; Cintas, A.; Miguez, H.; Serna, J. C.; Molpeceres, C.; Requena, J.; Mifsud, A.; Meseguer, F.; Lopez, C. *Langmuir* **1999**, *15*, 4701−4704.
(15) Rogach, A. L.; Kotov, N. A.; Koktysh, D. S.; Ostrander, J. W.; Ragoisha, G. A. *Chem. Mater.* **2000**, *12*, 2721−2726.
(16) Garcia-Santamaria, F.; Salgueirino-Maceira, V.; Lopez, C.; Liz-Marzan, L. M. *Langmuir* **2002**, *18*, 4519−4522.
(17) Jiang, P.; Bertone, J. F.; Hwang, K. S.; Colvin, V. L. *Chem. Mater.* **1999**, *11*, 2132−2140.
(18) Egen, M.; Zentel, R. *Chem. Mater.* **2002**, *14*, 2176−2183.
(19) Gu, Z.-Z.; Kubo, S.; Qian, W.; Einaga, Y.; Tryk, D. A.; Fujishima, A.; Sato, O. *Langmuir* **2001**, *17*, 6751−6753.
(20) Gu, Z.-Z.; Fujishima, A.; Sato, O. *Chem. Mater.* **2002**, *14*, 760−765.
(21) Picard, G. *Langmuir* **1998**, *14*, 3710−3715.
(22) van Duffel, B.; Ras, R. H. A.; De Schryver, F. C.; Schoonheydt, R. A. *J. Mater. Chem.* **2001**, *11*, 3333−3336.
(23) Stöber, W.; Fink, A.; Bohn, E. *J. Colloid Interface Sci.* **1968**, *26*, 62−69.
(24) Kang, S.; Hong, S. I.; Choe, C. R.; Park, M.; Rim, S.; Kim, J. *Polymer* **2001**, *42*, 879−888.

10.1021/cm021242w CCC: $25.00
Published on Web 01/03/2003

the silica particles are functionalized with allyltrimethoxysilane, a molecule that confers the silica particles a hydrophilic−hydrophobic balance, which is appropriate for the organization of the particles in a close-packed 2D array at the air−water interface. Several layers of silica particles are then successively transferred onto solid substrates. By adjusting the speeds of downstroke and upstroke of the substrate through the air−water interface, it is possible to transfer a single layer of particles at each cycle of the process. Consequently, colloidal crystals with a perfectly controllable thickness, that is, at the layer level, can be synthesized. In this work, up to 25 layers of silica particles have been deposited on substrates of various sizes and nature (attempts of transfer on glass slides, CaF_2, and mica sheets were successful). Finally, the colloidal crystals were observed with a scanning electron microscope and characterized with UV−visible−NIR spectroscopy to illustrate the degree of control of the sample thickness. Attempts to model experimental spectra with theoretical predictions based on the scalar wave approximation also gave satisfactory results.

Materials and Methods

Materials. Tetraethoxysilane (TEOS, Fluka), ammonia (25% in water, SDS), and allyltrimethoxysilane (ABCR) were purchased at reagent grade and used without further purification. Deionized water was obtained with a MilliQ system (Millipore) whereas ethanol and chloroform were purchased from J.T. Baker.

Methods. *Synthesis of Silica Particles.* The method employed for the synthesis of 460- and 680-nm silica particles was similar to the one described in a previous work.[25] First, given amounts of ethanol and ammonia solution were introduced into a three-neck round flask of 250 mL equipped with a refrigerating system. The mixtures were stirred at 300 rpm to homogenize them. Then, an ethanolic solution of TEOS was prepared separately and introduced continuously in the medium at a precise rate thanks to a single-syringe pump (see below). Reaction occurred at room temperature under continuous stirring for over 12 h.

reaction medium		solution of TEOS			
volume of ethanol (mL)	volume of ammonia (mL)	volume of ethanol (mL)	volume of TEOS (mL)	rate of addition (mL·h^{-1})	final particle size (nm)
200	22	40	10	8	460
100	22	40	10	8	680

Second, a large excess of allyltrimethoxysilane was added to functionalize the silica surface. The choice of this compound was driven by the following reasons. First, the surface of the particles should not be too hydrophilic, else an aggregation phenomenon occurs in the solution before spreading (see details below). In contrast, when the particles are too hydrophobic, the dispersion is easy but the particles aggregate at the air−water interface, which is confirmed by macroscopic observations. In both cases, the degree of organization of the particles at the interface is too low to form well-organized colloidal arrays. According to several attempts, not presented here, allyltrimethoxysilane is a good candidate for avoiding these problems. The minimal needed quantities were calculated assuming two hypotheses. First, a single molecule should cover a surface of 0.5 nm^2 as shown elsewhere.[26] Second, the total surface area of the particles is considered equal to the geometric surface developed by these particles. After several hours, the system was heated to 90 °C for 2 h to ensure the covalent attachment of the coupling agent on the surface of the silica particles. The involved quantities in the two syntheses are listed below (amounts were calculated for 1 g of silica in both cases).

silica particles		coupling agent		
diameter (nm)	surface developed (m^2)	amount required (mol)	volume required (μL)	volume added (μL)
460	5.93	1.97×10^{-6}	3.32	28.0
680	4.01	1.33×10^{-6}	2.24	18.6

Silica Suspensions Treatment. To eliminate the remaining reagents, all the suspensions were dialyzed against water several times and then transferred into a flask under continuous stirring. The final concentration of the suspension was determined by measuring the mass of a dried extract and the measured value was always in agreement with the theoretical one (calculated assuming a complete conversion of TEOS into silica).

Silica Particles Size Measurements. Granulometry experiments were performed on a Malvern Mastersizer apparatus.

Formation of a 2D Array of Particles. In a first step, a diluted suspension of functionalized silica particles in ethanol and chloroform was prepared. To increase the monodispersity of the silica particles, stirring of the suspension was stopped to allow the sedimentation of the particles.[27,28] Then, a few milliliters of the initial suspension were cautiously taken from the flask and transferred into a centrifugation tube. After the first centrifugation, which was rather fast considering the size and density of the particles, the supernatant was removed and the particles were redispersed in absolute ethanol. This operation was repeated several times to ensure a purification as complete as possible. Then, the particles were redispersed in a 80%/20% (v/v) mixture of chloroform and ethanol and sonicated for several minutes. Finally, this suspension was cautiously spread along the air−water interface of a Langmuir trough. Whereas the total area available was close to 0.4 m^2, the amount of spread particles was calculated in such a way that the surface coverage was close to 0.1 m^2 at the end of the process. To form the 2D particulate film, a stepwise compression of the particles was carried out with a mobile barrier until a surface pressure of ca. 10 mN·m^{-1}, that is, the pressure chosen for the transfer. Above this value, the film stability decreased quickly, suggesting the formation of 3D aggregates that were visible to the naked eye at the air−water interface.

Colloidal Crystal Synthesis. After compression, the Langmuir film was transferred onto solid substrates, consisting typically of hydrophilic glass slides. The slides were immersed quickly in the subphase (downstroke speed: 10 cm·min^{-1}) and then slowly pulled up out of the water (upstroke speed: 0.1 cm·min^{-1}). In these optimized conditions, for both sizes of particles, the deposition on the substrate only occurred during the upstroke with a transfer ratio close to unity, which allowed us to transfer a monolayer of particles at each cycle.

Scanning Electron Microscopy. SEM observations were performed with a JEOL JSM-840A scanning electron microscope operating at 10 kV. The specimens were gold-coated prior to examination.

UV−Visible/near-IR Spectroscopy. Experiments were performed with a Magna-IR Spectrometer 750 from Nicolet.

Results and Discussion

Colloidal Crystal Synthesis. To obtain colloidal crystals with the best possible quality through the LB

(25) Reculusa, S.; Poncet-Legrand, C.; Ravaine, S.; Mingotaud, C.; Duguet, E.; Bourgeat-Lami, E. *Chem. Mater.* **2002**, *14*, 2354−2359.
(26) Wescott, S. L.; Oldenburg, S. J.; Randall Lee, T.; Halas, N. J. *Langmuir* **1998**, *14*, 5396−5401.
(27) Ni, P.; Dong, P.; Cheng, B.; Li, X.; Zhang, D. *Adv. Mater.* **2001**, *13*, 437−441.
(28) Dimitrov, A. S.; Miwa, T.; Nagayama, K. *Langmuir* **1999**, *15*, 2557−5264.

technique, it is obvious that the elaboration of a 2D array of particles at the air−water interface is a key point. Considering other experiments not presented here, one can say that the organization at the interface is strongly dependent on the functionality and the size of the silica particles. Attempts at film formation with smaller silica particles (220 and 340 nm) also functionalized with allyltrimethoxysilane give unsatisfactory results since the particles apparently dive into the subphase when the pressure increases. When octyltriethoxysilane is used as a coupling agent, the particles form macroscopic aggregates at the interface during the spreading. These aggregates may be well-organized over short distances but they are too rigid to reorganize themselves during the compression and then cannot lead to a uniform 2D array at the trough scale.

In the present study, values of downstroke and upstroke speeds of the substrates through the interface were adjusted to transfer a single layer of particles per cycle. Two modes only were available for the downstroke (0.1 and 10 cm·min^{-1}), whereas the upstroke speed was adjustable in the range 0.01−10 cm·min^{-1}.

In the slow downstroke mode, the particles already deposited have a tendency to spread again at the interface, which can be inferred from the mobile barrier movement (area increases whereas surface pressure remains the same). In the fast mode, the substrate dives quickly in the subphase and the problem is avoided.

In the same time, several values of upstroke speed have been tested for the transfer of a single layer of particles. For the higher speeds (>0.1 cm·min^{-1}), calculated transfer ratios are inferior to 1; that is, the substrate is not fully covered with particles, which is visible to the naked eye. On the other hand, no difference was observed for speeds between 0.01 and 0.1 cm·min^{-1} since the transfer ratios are close to 1 and the particles are uniformly deposited. To optimize the process and the time consumed, the value of upstroke speed was consequently taken equal to 0.1 cm·min^{-1}.

Initially, rate deposition of the particles during the transfer could strongly depend on the interactions between the substrate and the liquid film of particles. Complementary attempts have been carried out to transfer differently functionalized silica particles (either with hydrophilic or hydrophobic groups) onto hydrophobic substrates, like glass slides previously treated with trimethylchlorosilane or plastic slips. Since they all proved to be unsuccessful, one can neglect the influence of the particle−substrate interactions and consider the substrate−subphase interactions as a determining parameter in the process.

Water being the subphase in our case, experiments with hydrophilic substrates such as CaF_2 or mica sheets led to good transfer ratios. This obviously indicates that a good wetting of the substrate surface by the liquid film of particles is required to obtain a correct result. In the present work, all the substrates used are microscope slides (2.5 × 2.5 cm) consisting of hydrophilic glass. To improve the hydrophilic character, preliminary treatments with sulfochromic acid may also be considered.

Transferring onto a glass slide a single layer of silica particles is a good way to illustrate the quality of the organization at the surface of the Langmuir trough. As can be seen in Figure 1, observation of the sample by SEM at low magnification shows that the particles are close packed in a hexagonal lattice with some local defects and grain boundaries.

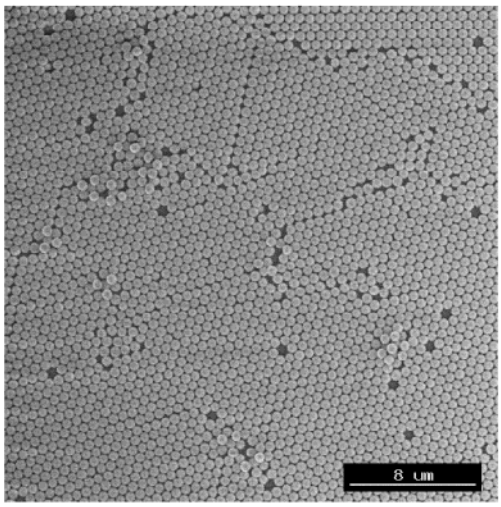

Figure 1. Top view of a single layer of silica particles (diameter: 680 nm) transferred onto a glass slide.

However, as shown in Figure 2, the arrangement of the particles is regular over 100-μm^2 sections for both sizes of particles. FFT images presented as insets in this figure are also significant of the long-range order, which is visible to the naked eye since the samples are iridescent.

In Figure 3 are presented side views of colloidal crystals synthesized through successive depositions (3, 5, 10, and 25 layers, respectively) of 680-nm silica particles.

Although not represented here, the structures obtained with silica particles with a diameter around 460 nm are perfectly similar. As can be seen, the number of deposited layers that one can easily count matches perfectly with the predefined number of transfer cycles. Thickness is quite uniform and the upper layer remains well-organized. As shown in Figure 4 for the thickest sample, there are some sphere vacancies and vertical cracks due to both the high vacuum exposure during observation and the drying-induced shrinkage.

However, the overall quality is obviously good enough to allow the deposition of complete layers of particles during the following cycles.

Sample Analysis. As is widely described elsewhere, near-IR and UV−visible spectroscopies are interesting techniques for characterizing the optical properties of such colloidal crystals.[29,30] In this work, we have recorded experimental spectra in the range 4000−15000 cm^{-1}. In all the spectra, shown in Figure 5, we observe one main peak corresponding to the Bragg diffraction according to the well-known Bragg's law,

$$m\lambda_m = \lambda_B = 2n_e d_{hkl} \sin \alpha_B \qquad (1)$$

(29) Goldenberg, L. M.; Wagner, J.; Stumpe, J.; Paulke, B.-R.; Görnitz, E. *Langmuir* **2002**, *18*, 3319−3323.

(30) Miguez, H.; Lopez, C.; Meseguer, F.; Blanco, A.; Vazquez, L.; Mayoral, R.; Ocana, M.; Fornes, V.; Mifsud, A. *Appl. Phys. Lett.* **1997**, *71*, 1148−1150.

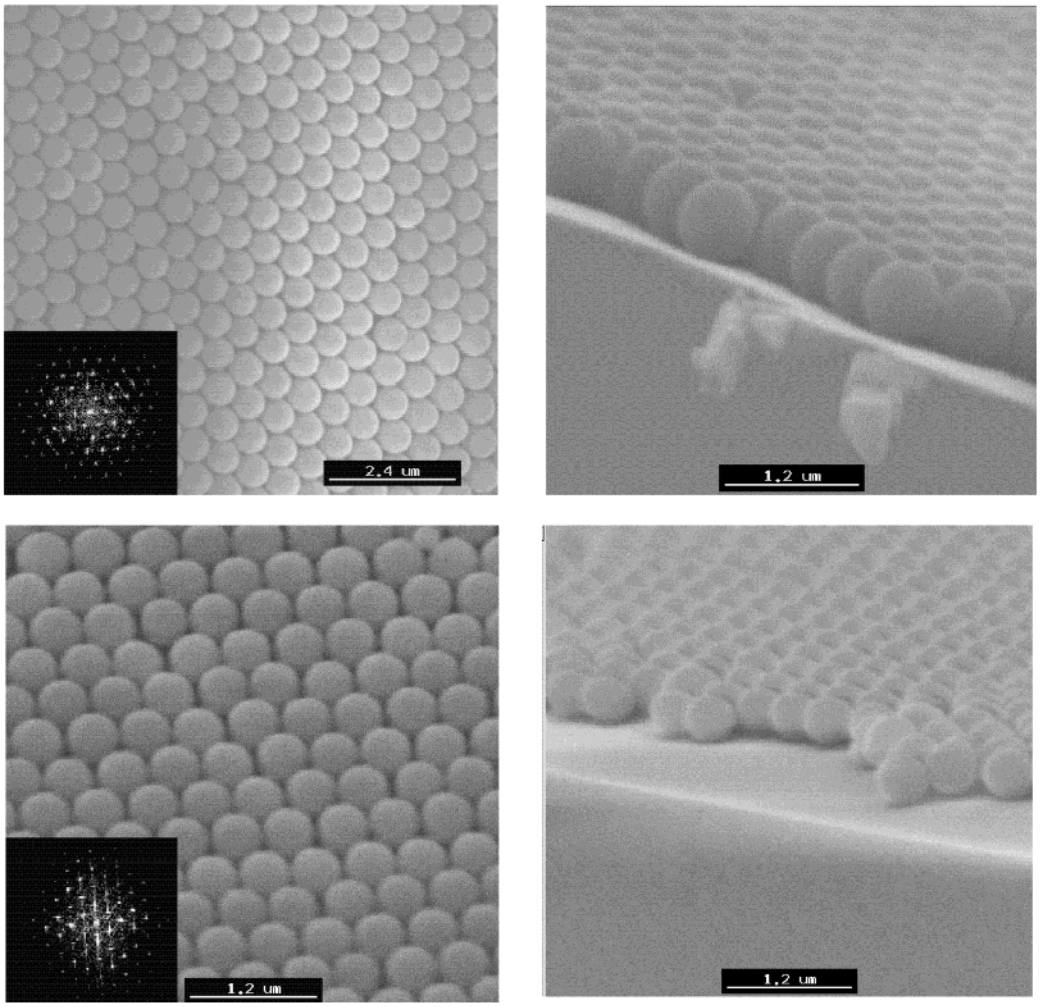

Figure 2. Top and side views of monolayers of functionalized silica particles (diameters: 680 nm, top, and 460 nm, bottom) transferred onto a glass substrate by the Langmuir−Blodgett technique.

where m is an integer (corresponding to the diffraction order), λ_B is the Bragg diffracted wavelength, n_e is the effective refractive index of the crystal, d_{hkl} is the distance between two consecutive lattice planes with Miller indices (h,k,l), and α_B is the Bragg angle.

In our experimental conditions, the diffracted intensity is measured in the same direction as the incident beam, which is itself perpendicular to the surface of the crystal.

Consequently, assuming that we have a fcc lattice, we are in the condition of the Bragg diffraction angle ($\alpha_B = 90°$) for the lattice planes with Miller indices (1,1,1). Modifying eq 1, it comes that the main peak corresponding to the first order of diffraction ($m = 1$) is obtained when

$$\lambda = \lambda_B = 2n_e d_{111}$$

In the case of a fcc lattice consisting of spheres of a diameter D, the value of d_{111} is given by

$$d_{111} = \sqrt{\frac{2}{3}} \times D$$

and the effective refractive index n_e is calculated using indices of silica (n_s) and air (n_a) and the volume fraction ϕ (0.74 for closely packed spheres) occupied by the silica spheres according to

$$n_e = \sqrt{\phi {n_s}^2 + (1 - \phi){n_a}^2}$$

Therefore, the particles diameter can be calculated from the Bragg peak position (see results in Table 2).

In the experimental transmission spectra (see Figure 5), we also observe several peaks known as Fabry-Pérot fringes for wavelengths higher than λ_B due to interferences between beams transmitted and partially reflected at the silica−air and silica−glass interfaces.

In a first approximation, the system can be considered as a layer of index n_e and of thickness θ deposited on a glass substrate. Considering that the incident beam has an amplitude a_0, we can estimate the amplitude of each beam emerging from the colloidal crystal layer,

$$a_i = a_0(t_1 t_2)(r_1 r_2)^{i-1} = a_0 T R^{i-1}$$

where t_1 and r_1 (t_2 and r_2) are the transmission and reflection coefficients for the air-silica (silica-glass) interface and a_i is the amplitude of the ith emerging beam. If we now take into account the complex expression of the amplitudes, a_i, we have to consider the

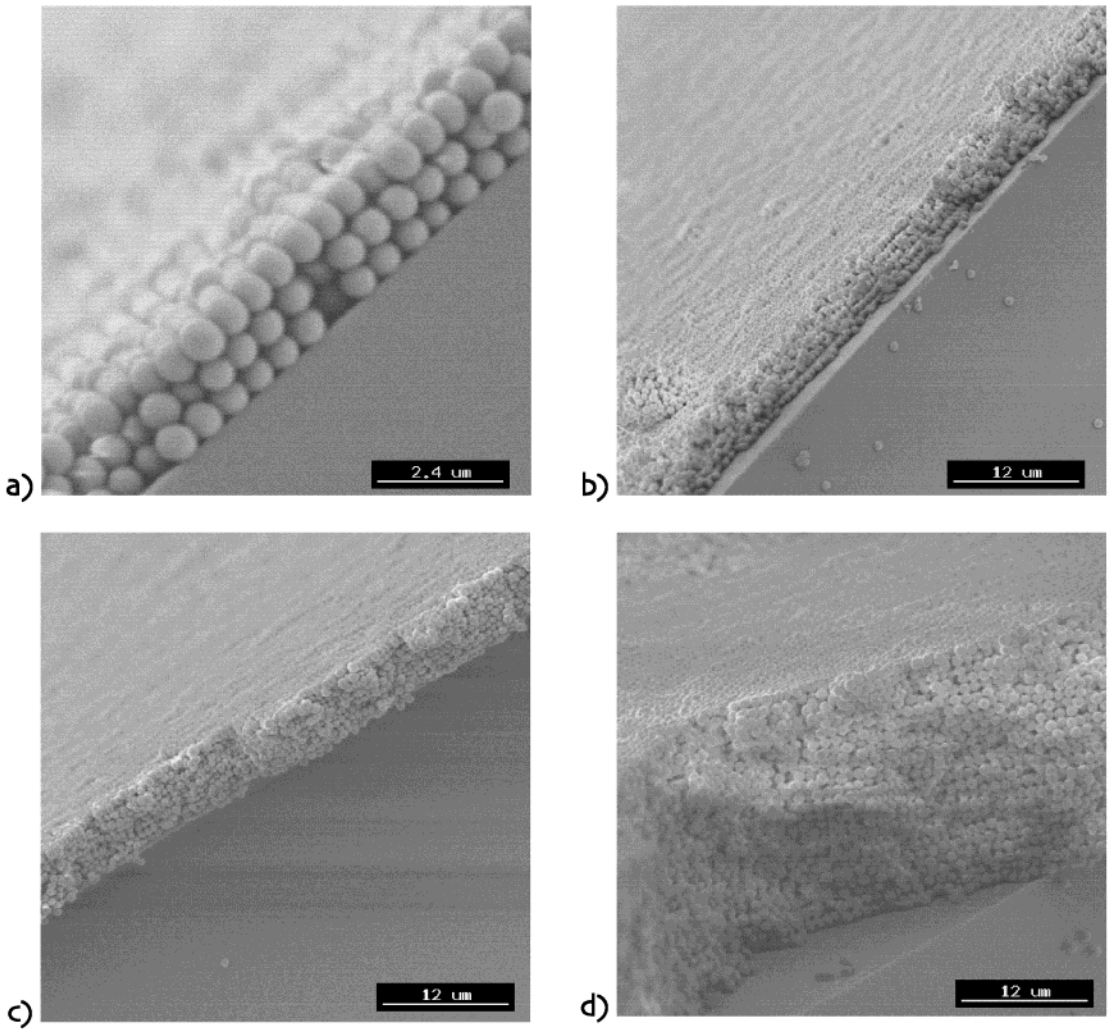

Figure 3. Side views of colloidal crystals consisting of several layers of silica particles (diameter 680 nm). The pictures illustrate the results of the multistage deposition for 3, 5, 10 and 25 layers.

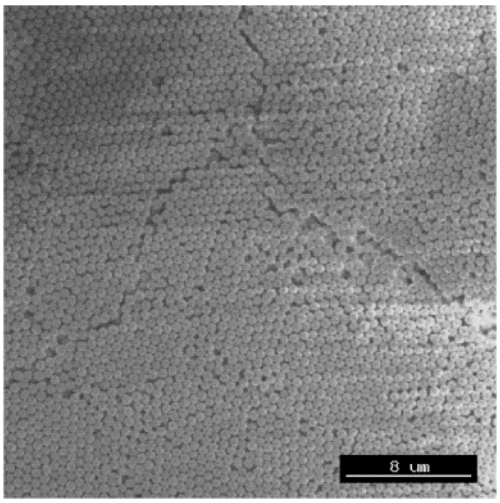

Figure 4. Upper surface of a 25-layer sample (particle diameter: 680 nm).

difference of optical pathways between two different beams,

$$a_i = a_i(\mathrm{e}^{-j(i-1)\varphi}) = a_i(\mathrm{e}^{-j\varphi})^{i-1}$$

where φ is the difference of optical pathways between two consecutive rays related to the difference of geometrical pathways δ given by

$$\varphi = \frac{2\pi}{\lambda} \times \delta$$

and

$$\delta = 2n_e\theta \cos i$$

where i is the angle of incidence of the beam on the sample (equal to 0 in our case).

Considering a perfect fcc crystal, the thickness θ is directly related to the number of deposited layers, N, according to the following nonlinear expression:

$$\theta(N) = \left[1 + \left((N-1) \times \sqrt{\frac{2}{3}}\right)\right] \times D \qquad (2)$$

The resulting amplitude, A, is given by the following:

$$A_n = \sum_{k=1}^{n} a_k = a_1 \times \sum_{k=1}^{n} R^{k-1}(\mathrm{e}^{-j\varphi})^{k-1} = a_1 \times \sum_{k=0}^{n-1}(R\mathrm{e}^{-j\varphi})^k$$

and

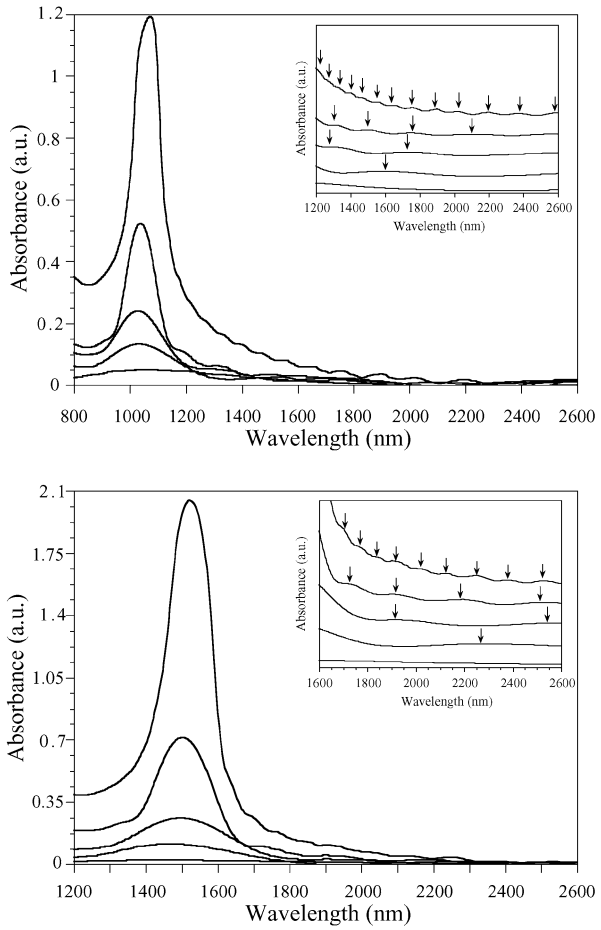

Figure 5. Experimental UV−visible−NIR transmission spectra obtained with colloidal crystals based on silica particles of different diameters (460 nm, top, and 680 nm, bottom). On each graph are given the results for several numbers of layers (1, 3, 5, 10, and 25 layers from bottom to top) whereas the insets show the positions of the Fabry-Pérot fringes.

$$A = \lim_{n \to +\infty} A_n = \frac{a_0 T}{1 - R e^{-j\varphi}}$$

Finally, the transmitted intensity, I_t, is given by

$$I_t \propto A\, A^* = \frac{{a_0}^2 T^2}{1 - R^2} \times \frac{1}{1 + \frac{4R}{1 - R^2} \times \left(\sin \frac{\varphi}{2}\right)^2}$$

and while considering the incident intensity I_0, one can write

$$\frac{I_t}{I_0} \propto \frac{1}{1 + \gamma \times \left(\sin \frac{\varphi}{2}\right)^2}$$

where

$$\gamma = \frac{4R}{1 - R^2}$$

The absorbance of the sample, Abs, defined as

$$\mathrm{Abs} = -\log\left(\frac{I_t}{I_0}\right)$$

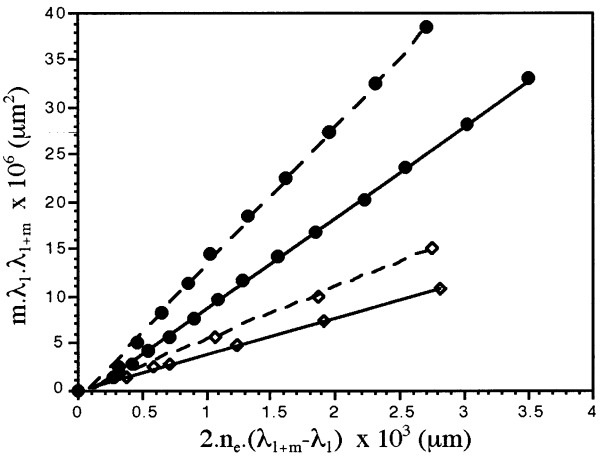

Figure 6. Experimental values of $m\lambda_1\lambda_{1+m}$ plotted as a function of $2n_e(\lambda_{1+m} - \lambda_1)$ and corresponding linear fits. Thicknesses were calculated for two different sizes of silica particles (continuous line, 460 nm; dotted line, 680 nm) and two different numbers of layers (◇, 10 layers; ●, 25 layers).

reaches a maximum when the denominator of the above function is maximal, which occurs when

$$|\sin\frac{\varphi}{2}| = 1 \leftrightarrow \varphi \equiv \pi[2\pi] \leftrightarrow \frac{4n_e\theta}{\lambda} = 2p + 1$$

where p is an integer.

While considering two values of the wavelength, λ_p and λ_{p+m}, for which the absorbance is maximal, it is then possible to estimate the value of the thickness θ. Indeed,

$$4n_e \times \frac{\theta}{\lambda_p} = 2p + 1; \qquad 4n_e \times \frac{\theta}{\lambda_{p+m}} = 4n_e \times \frac{\theta}{\lambda_p} + 2m$$

Consequently,

$$m\lambda_p\lambda_{p+m} = 2n_e(\lambda_{p+m} - \lambda_p)\theta \qquad (3)$$

Insets in Figure 5 illustrate the positions of the Fabry-Pérot fringes for all the samples (values of absorbance relative to different thicknesses were adjusted arbitrarily for a better viewing). As expected, the higher the number of layers (and so the thickness), the higher the number of fringes. In all the cases, the experimental values were taken considering $\lambda_p = \lambda_1$, that is, the wavelength corresponding to the first fringe observable after the Bragg peak. From eq 3, it is obvious that the plot of $m\lambda_p\lambda_{p+m}$ versus $2n_e(\lambda_{p+m} - \lambda_p)$ should be a linear curve with a slope equal to the thickness θ of the sample. Figure 6 illustrates the result of the calculations for the two sizes of silica particles with numbers of layers of 10 and 25, that is, when the number of experimental values is significant enough. As expected, the graphs exhibit a well-defined linear behavior.

Finally, the theoretical diameters of the silica particles are calculated starting from the so-estimated values of the thickness and using eq 2. The results given in Table 1 are in good agreement with the values already estimated by granulometry or calculated from the Bragg peak position.

Many theories have already been developed along the influence of photonic band structures on diffraction

Table 1. Values of Diameters of Silica Particles Estimated from the Positions of Fabry-Pérot Fringes for Four Different Samples

	experimental thickness (μm)		calculated particle diameter (nm)	
	$N = 10$	$N = 25$	$N = 10$	$N = 25$
size 1	3.872	9.680	464	470
size 2	5.557	14.604	666	709

patterns of colloidal crystals.[31−33] Two approaches known as the scalar wave approximation (SWA) and the dynamical diffraction theory (DDT) that take into account the periodicity of the medium are commonly used to describe the behavior of these crystals. As described by Mittleman et al., these models consist of rather simple analytic expressions but can lead to good agreement with the experimental data, either the full transmission spectrum or more specific characteristics such as the position and the width of the peaks.[34,35] Shortly, in the SWA case, the electric field is considered like a scalar quantity and in the DDT approach, the electric field remains a vector quantity but the refractive index of the crystal is considered equal to 1, which is a bit restrictive. However, in both theories, the contribution of a single set of lattice planes is taken into account to calculate the diffracted intensity. In our case, we have used the SWA theory to simulate the UV−visible−NIR transmission spectra.

As detailed by Shung and Tsai,[31] it is possible to solve the Maxwell equation for an electric field in a periodic medium, where the dielectric function is the sum of an average dielectric constant ϵ_0 and a periodic part ϵ'. The solutions of such a system depend on the sign of a function $F(\omega)$ given by

$$F(\omega) = \frac{G^2}{4} + \epsilon_0 \times \left(\frac{\omega}{c}\right)^2 - \sqrt{G^2 \times \epsilon_0 \times \left(\frac{\omega}{c}\right)^2 + {U_G}^2 \times \left(\frac{\omega}{c}\right)^4}$$

where $G = 2\pi/d_{111}$ is a reciprocal wave vector and U_G the corresponding Fourier coefficient in the Fourier development of the periodic function ϵ'.[31,34]

When the system resulting from the Maxwell equations is resolved, nontrivial solutions with the following general expression are found:

$$k = \frac{G}{2} \pm q \quad \text{in band regions where } F(\omega) \geq 0$$

or

$$k = \frac{G}{2} \pm iq \quad \text{in gap regions where } F(\omega) \leq 0$$

with $q = \sqrt{F(\omega)}$

Finally, the transmission rate is calculated after considering the limit conditions (continuity of $E(x)$ and its first derivative at the interfaces) and can be expressed as follows:

$$\frac{I_t}{I_0} = T = \begin{cases} \dfrac{1}{1 + (\kappa_b - 1) \times \sin^2(kNd_{111})} & \text{in band regions} \\ \dfrac{1}{1 + (\kappa_g + 1) \times \sinh^2(qNd_{111})} & \text{in gap regions} \end{cases}$$

where κ_b and κ_g are analytic expressions depending on other parameters not described here (see ref 28 for more details). Values of absorbance can then easily be estimated since Abs $= -\log(T)$.

These expressions of T were employed to fit the experimental transmission spectra of the thickest samples (i.e., with a maximal number of fringes). Results of the fitting procedure, carried out with N equal to 25 and with d_{111} as only adjustable parameter, are shown in Figure 7. For better clarity, theoretical graphs were corrected in such a way as values of maxima at the Bragg peak wavelength are equal. As shown in the insets, the coincidence between the fringe positions is almost perfect, taking into account that no baseline correction was carried out for the experimental spectra.

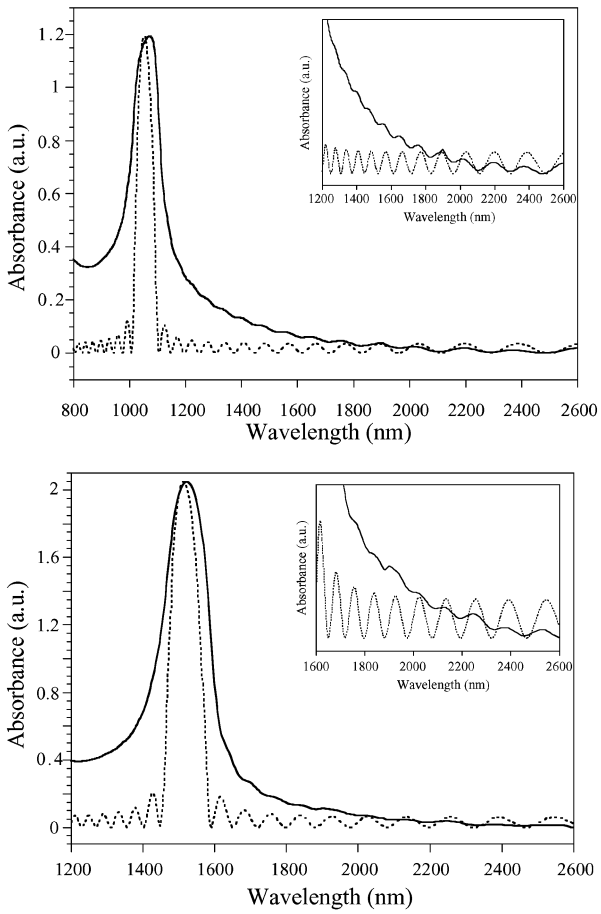

Figure 7. Comparison between experimental (continuous lines) and predicted (dotted lines) UV−visible−NIR spectra for colloidal crystals consisting of 25 layers of silica particles (diameter: 460 nm, top, and 680 nm, bottom). Insets illustrate the concordance of the peaks in the range of wavelengths where Fabry-Pérot fringes appear.

(31) Shung, W.-K.; Tsai, Y. C. *Phys. Rev. B* **1993**, *48*, 11265−11269.
(32) Vos, W. L.; Sprik, R.; van Blaaderen, A.; Imhof, A.; Lagendijk, A.; Wegdam, G. H. *Phys. Rev. B* **1996**, *53*, 16231−16235.
(33) Satpathy, S.; Zhang, Z.; Salehpour, M. R. *Phys. Rev. Lett.* **1990**, *64*, 1239−1242.
(34) Mittleman, D. M.; Bertone, J. F.; Jiang, P.; Hwang, K. S.; Colvin, V. L. *J. Chem. Phys.* **1999**, *111*, 345−354.
(35) Bertone, J. F.; Jiang, P.; Hwang, K. S.; Mittleman, D. M.; Colvin, V. L. *Phys. Rev. Lett.* **1999**, *83*, 300−303.

Table 2. Comparison of the Average Values of the Silica Particles Diameters (nm) Estimated with Several Techniques

	granulometry	Bragg peak position	Fabry-Pérot fringes	SWA model
size 1	460	477	467	480
size 2	680	686	688	690

The corresponding values of D, calculated from d_{111} given by the model, are listed in Table 2. This time again, good agreement with the diameters calculated by other techniques is achieved, which is significant of both the quality of the initial silica particles and more generally their organization in the colloidal crystal.

Compared to other techniques of elaboration, the main advantage of the procedure we have studied is that it offers control of the sample thickness at the particle layer level. For a 1-cm-height substrate, the process takes 15 min for a single layer (10 for the upstroke and 5 to allow the Langmuir film to reorganize itself and the substrate to dry). Whether it may be a little bit more time-consuming than the convective assembly method, it is still much faster than processes involving evaporation or sedimentation. On the other hand, the technique may be of interest if one intends to obtain colloidal crystals with particles more expensive or difficult to synthesize than silica. The needed amount of particles is indeed very low compared to convective assembly, which usually requires concentrated suspensions of particles.

Conclusion

We have demonstrated that appropriately functionalized silica particles of various diameters can be organized in colloidal crystals through the Langmuir−Blodgett technique. The main advantage of this approach is that a perfect control of the thickness (at the layer level) of the crystal is obtained in a very reasonable scale of time.

SEM observations both illustrate the high degree of organization of the silica particles at the interface and the matching between experimental and theoretical numbers of deposited layers, from 1 up to 25. Spectroscopic data, consisting of UV−visible−NIR spectra, show that both Bragg peak and Fabry-Pérot fringes positions allow calculation of the diameter of the particles, which is in good agreement with the granulometry and SEM measurements. Theoretical simulations of the experimental spectra using a model based on the scalar wave approximation also led to satisfactory results.

We are currently carrying out further experiments with smaller and bigger particles, and we hope to give evidence that the technique can be extended to other sizes and systems.

Acknowledgment. The authors would like to thank Béatrice Agricole (CRPP, Pessac) and Elisabeth Sellier (CREMEM, Talence) for their precious help in the Langmuir experiments and SEM observations, respectively.

Note Added after ASAP Posting

This article was released ASAP on 1/3/2003 with a misspelling in one of the authors' names. The correct version was posted the same day.

CM021242W